Comparative Study of Advanced Signal Processing Techniques for Islanding Detection in a Hybrid Distributed Generation System

Soumya R. Mohanty, *Senior Member, IEEE*, Nand Kishor, *Senior Member, IEEE*, Prakash K. Ray, *Member, IEEE*, and João P. S. Catalão, *Senior Member, IEEE*

***Abstract*—In this paper, islanding detection in a hybrid distributed generation (DG) system is analyzed by the use of hyperbolic S-transform (HST), time–time transform, and mathematical morphology methods. The merits of these methods are thoroughly compared against commonly adopted wavelet transform (WT) and S-transform (ST) techniques, as a new contribution to earlier studies. The hybrid DG system consists of photovoltaic and wind energy systems connected to the grid within the IEEE 30-bus system. Negative sequence component of the voltage signal is extracted at the point of common coupling and passed through the above-mentioned techniques. The efficacy of the proposed methods is also compared by an energy-based technique with proper threshold selection to accurately detect the islanding phenomena. Further, to augment the accuracy of the result, the classification is done using support vector machine (SVM) to distinguish islanding from other power quality (PQ) disturbances. The results demonstrate effective performance and feasibility of the proposed techniques for islanding detection under both noise-free and noisy environments, and also in the presence of harmonics.**

***Index Terms*—Distributed generation (DG), islanding detection, power quality (PQ), signal processing, support vector machine (SVM).**

I. Introduction

ALTHOUGH there is a huge expansion of transmission and distribution of power supply, it is still inadequate to meet the scarcity of the power demand. In this context, penetration of renewable energy resources-based distributed generation (DG) is gradually increasing, which seems a suitable alternative.

However, due to the intermittency in wind speed and solar radiation intensity, they can be integrated with fuel cells along with other storage systems to constitute a hybrid system for reliable and improved power quality (PQ) [1], [2]. On the other hand, high penetration of such systems raises serious issues related to islanding occurrence events and PQ problems that need to be addressed [3].

Islanding is a phenomenon that occurs when DG resources feed to the local load and the utility grid is disconnected. Accurate and early detection of these disturbances is very important to improve the operation of DG systems. In the past few years, a number of research papers have been reported.

Islanding detection techniques can be categorized into active and passive methods [4]. Usually, active methods are based on the injection of a small disturbance into the system and analyzing the change in output parameters for islanding detection. Some of the popular active detection techniques are Sandia frequency shift (SFS), active frequency drift (AFD) [5], automatic phase shift (APS), and slip mode frequency shift (SMS) [6]. Although these methods provide less nondetection zone (NDZ), SFS may lead to poor PQ because of positive feedback, while AFD, APS, and SMS may show higher NDZ with an increase of reactive load. Passive methods require monitoring of system parameters and the selection of a suitable threshold in order to detect an islanding event. In fact, challenges exist in selecting the most significant parameters and an appropriate threshold value. The use of voltage unbalance/total harmonic distortion (VU/THD) methodology may cause undesirable trip signal to the circuit breaker due to accumulated sum over the performance indices within one cycle of load switching, which may be misinterpreted as islanding [7], [8]. The rate of change of frequency (ROCOF) [9], [10] has also been considered for the detection of islanding events. Nonetheless, with the variation of real and reactive power imbalance, this method may lead to NDZ [11]. Intelligent-based techniques for islanding detection are discussed in [12] based on the variations in system parameter indices and data-mining technology. Then, the transient characteristic of disturbance signals is utilized for detecting power islands [13], [14].

Nevertheless, to minimize NDZ in the above-mentioned methods, signal processing techniques like short-time Fourier transform (STFT), wavelet transform (WT), S-transform (ST), hyperbolic S-transform (HST), and time-time (TT) transform (TTT) [15]–[18] are being considered to improve detection performance. Brief time–frequency characteristics can be conveniently achieved by using STFT, but the transient signals

Manuscript received February 16, 2014; revised June 17, 2014 and September 11, 2014; accepted October 05, 2014. The work of J. P. S. Catalão was supported by FEDER funds (European Union) through COMPETE and from Portuguese funds through FCT-Portugal, under Projects FCOMP-01-0124-FEDER-020282 (PTDC/EEA-EEL/118519/2010) and PEst-OE/EEI/LA0021/2013. Paper no. TSTE-00069-2014.

S. R. Mohanty and N. Kishor are with the Motilal Nehru National Institute of Technology, Allahabad 211004, India (e-mail: soumya@mnnit.ac.in; nand_research@yahoo.co.in).

P. K. Ray is with the International Institute of Information Technology, Bhubaneswar 751003, India (e-mail: pkrayiiit@gmail.com).

J. P. S. Catalão is with the University of Beira Interior, 6201-001 Covilha, Portugal, with the Instituto de Engenharia de Sistemas e Computadores—Investigação e Desenvolvimento (INESC-ID), 1000-029 Lisbon, Portugal, and also with the Instituto Superior Técnico (IST), University of Lisbon, 1049-001 Lisbon, Portugal (e-mail: catalao@ubi.pt).

Color versions of one or more of the figures in this paper are available online at http://ieeexplore.ieee.org.

Digital Object Identifier 10.1109/TSTE.2014.2362797

cannot be adequately described due to its fixed window size. Again, wavelet is a strong candidate for classification scheme to analyze the signal signature, but is oversensitive to noise signals and involves computational complexity. The extension of WT with phasor information, known as ST [17], [18], was developed for the detection of various islanding and PQ disturbances, based on moving a varying and scalable localizing Gaussian window [19], [20]. However, in some nonstationary signals accompanied with transients, the detection capability of ST also degrades [21].

Therefore, considering the review of available techniques reported in the literature, the study in this paper considers a modified version of ST, i.e., HST, to compare with WT and ST for islanding detection. TTT [22]–[24] that represents time–time resolution is also used in the comparative study. These techniques are applied to extract more distinctive and pertinent statistical features, such as standard deviation (STD), energy and cumulative-sum (CUSUM) with selection of an appropriate threshold value, so that islanding events are localized. Moreover, mathematical morphology with simple addition and subtraction operator [25]–[27] is also explored in this paper for islanding detection.

Hence, as a new contribution to earlier studies, a plethora of techniques (HST, TTT, and mathematical morphology, against WT and ST) along with support vector machine (SVM) is proposed and studied in a comprehensive way for islanding detection and classification of disturbances under various operating scenarios.

This paper is organized as follows. The DG-based hybrid IEEE 30-bus system is introduced in Section II. Islanding detection methods are given in Section III. The simulation results with the comparative study of detection methods performance are provided in Section IV. Finally, the conclusion drawn from the study is presented in Section V.

II. DG-Based Hybrid System

Alternative energy resources, such as photovoltaic, wind energy systems, and fuel cells have gained momentum with penetration in the main grid to meet the scarcity of power to a greater extent. But, the intermittent nature of both wind speed and solar radiation intensity affects the reliability of power supply.

In this context, integration of the resources to form a hybrid DG system becomes a suitable alternative in order to minimize the problems. The system may be connected to the grid to share the excess or deficit power, as per situation demands.

Fig. 1 shows the IEEE 30-bus hybrid DG system to study the effect of wind/photovoltaic penetration on the detection of islanding event.

This system consists of three wind generators denoted as DG1 to DG3, and a photovoltaic system denoted as DG4. The modeling of the wind energy system, and photovoltaic system, with their specifications, in the current study is referred in [2] and [18].

The overall specifications of this system are as follows.

1) *Generator*: rated short-circuit 1200 kVA, 50 Hz, and 11 kV.

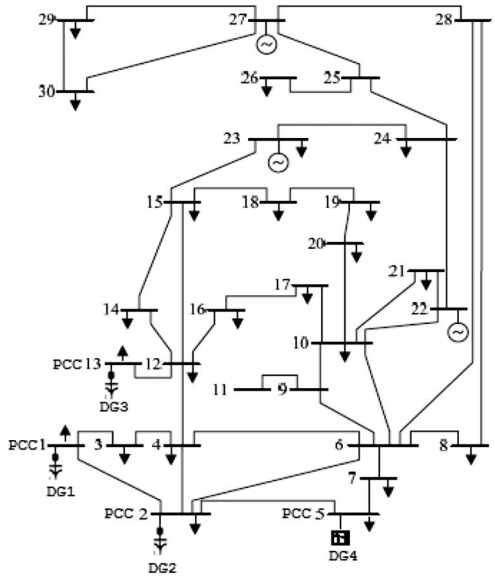

Fig. 1. IEEE 30-bus hybrid system with wind and photovoltaic penetration.

2) *DG*:
   a) DG1, DG2, and DG3: wind generators with 200 kW each, 500 V, doubly-fed induction generator type.
   b) DG4: photovoltaic system with 100 kW, 500 V.
   c) Boost converter: switching frequency of 8 kHz, input dc voltage of 200 V, output ac of 500 V, line-to-line.
   d) Loads: 150 kW (at DG1, DG2, and DG3), 80 kW (at DG4).

III. Islanding Detection Methods

This section presents a brief description of the signal processing techniques used for islanding detection.

The application of wavelet and ST was already demonstrated in [18] and [19] and thus not discussed here.

The following sections describe HST, TTT, and mathematical morphology that are explored in this paper for islanding detection. Fig. 2 shows the flowchart for islanding detection.

A. Hyperbolic S-Transform

The phasor information on contrary to WT is provided for the detection of signatures in time–frequency plane. Yet, the localization is carried out by fixed Gaussian window that has no parameter variation with respect to time/frequency and thus sometimes degrade its performance [21].

On the other hand, ST with Gaussian window fails to localize disturbances in time domain, while its variant known as HST that has pseudo-Gaussian hyperbolic window offers greater control over the window function, providing better time and frequency resolutions at low and high frequencies. The hyperbolic window provides frequency dependence shape along with its width and height. A higher asymmetry of the window at low frequencies leads to an increase in width in the frequency domain, with consequent interference between dominant noise frequencies [21].

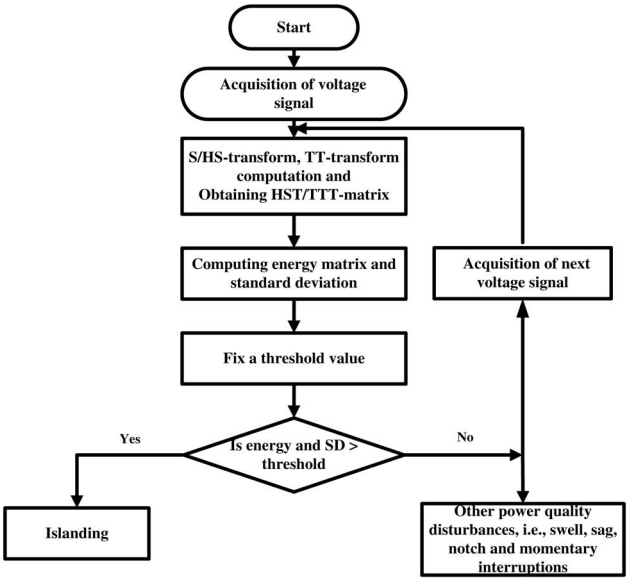

Fig. 2. Flowchart for islanding and PQ disturbance detection using ST, HST, and TTT.

In this study, HST contour is used for islanding detection where the hyperbolic window is defined as

$$W_{\rm hb} = \frac{2f_s}{\sqrt{2\pi\left(\alpha_{\rm hb}+\beta_{\rm hb}\right)}}\exp\left\{-\frac{-f_s^2X^2}{2}\right\} \tag{1}$$

where

$$X = \frac{(\alpha_{\rm hb}+\beta_{\rm hb})}{2\alpha_{\rm hb}\beta_{\rm hb}}(\tau-t-\xi) + \frac{(\alpha_{\rm hb}-\beta_{\rm hb})}{2\alpha_{\rm hb}\beta_{\rm hb}}\sqrt{(\tau-t-\xi)^2+\lambda_{\rm hb}^2}$$

$$0<\alpha_{\rm hb}<\beta_{\rm hb} \quad \text{and} \quad \xi = \frac{\sqrt{(\beta_{\rm hb}-\alpha_{\rm hb})^2\lambda_{\rm hb}^2}}{4\alpha_{\rm hb}\beta_{\rm hb}}. \tag{2}$$

The discrete version of HST can be calculated, and $G(m_F, n_F)$ denotes Fourier transform of hyperbolic window

$$G(m_F,n_F) = \frac{2f_s}{\sqrt{2\pi(\alpha_{\rm hb}+\beta_{\rm hb})}}\exp\left\{-\frac{-f_s^2X_D^2}{2}\right\} \tag{3}$$

where

$$X_D = \frac{(\alpha_{\rm hb}+\beta_{\rm hb})}{2\alpha_{\rm hb}\beta_{\rm hb}}t + \frac{(\alpha_{\rm hb}-\beta_{\rm hb})}{2\alpha_{\rm hb}\beta_{\rm hb}}\sqrt{t^2+\lambda_{\rm hb}^2}. \tag{4}$$

$H[m_F, n_F]$ is the frequency-shifted Fourier transform, $H[m_F]$ which is given by

$$H[m_F] = \frac{1}{N}\sum_{m_F=0}^{N-1} h(k)\exp(-i2\pi n_F k) \tag{5}$$

$$S[n_F, j] = \sum_{m_F=0}^{N-1} H(m_F+n_F)G(m_F,n_F)\exp(-i2\pi m_F j) \tag{6}$$

where N is the total number of samples and $G(m_F, n_F)$ represents the Fourier transform of the hyperbolic window.

B. TTT

The computation of inverse Fourier transform of discrete ST provides discrete TTT that maps single-dimensional signal in time domain to two-dimensional signal in time domain.

Since each of these is associated with a particular window position on the time axis, collectively they give a time–time distribution. The selection of different level as in WT is not required in the TTT. Further, high-frequency component of the signal is better localized in TTT and its output. In this technique, among the different frequency components, the high-frequency components have more energy concentration, thus leading to better localization property. One of the major utility of the TTT is the time-local view, through the scaled windows of the primary time series that makes it an appropriate approach for disturbance detection [22]–[24].

The Fourier transform of the signal is taken as a window sliding along the time axis. Hence, it is designated as the two-dimensional representation of the signal. The general expression of short-time Fourier transform is given by

$$\mathrm{STFT}(t,f) = \int_{-\infty}^{\infty} h(\tau)w(t-\tau)\exp(-2\pi i f\tau)d\tau. \tag{7}$$

By applying the inverse FT of (7) brings

$$[h(\tau)w(t-\tau)] = \int_{-\infty}^{\infty} \mathrm{STFT}(t,f)\exp(-2\pi i f\tau)df. \tag{8}$$

When all values of t are considered, the window function $h(\tau)w(t-\tau)$ becomes a two-dimensional function denoted by $\mathrm{STFT}_{\rm TT}$, given by

$$\mathrm{STFT}_{\rm TT}(t,\tau) = \int_{-\infty}^{\infty} \mathrm{STFT}(t,f)\exp(2\pi i f\tau)df. \tag{9}$$

TTT is obtained from ST as

$$\mathrm{TT}(t,\tau) = \int_{-\infty}^{\infty} S(t,f)\exp(2\pi i f\tau)df. \tag{10}$$

The discrete form appears as

$$\mathrm{TT}(k\Delta t, j\Delta t) = \sum_{n=N/2}^{N/2-1} S(n\Delta f, j\Delta t)\exp(i2\pi nk/N) \tag{11}$$

$$h(k_t\Delta t) = \sum_{j=0}^{N-1} \mathrm{TT}(k_t\Delta t, j\Delta t) \tag{12}$$

where Δt is the time interval, N is the sampling number, k_t is the time index, $k_t = 0, 1, \ldots, N-1$, j is the time shifting index, and n_F is the frequency index.

C. Mathematical Morphology

Morphological filters are nonlinear signal transformation tools that modify shapes of signals [25]. Mathematical morphology is developed from set theory and integral geometry,

and derives its name because it deals with the shape of signals. It is a nonlinear signal processing approach applied to the study on power system fault/disturbance.

The wavelet, HST, and TTT are all used as integral transform for detection objective. In fact, computational complexity is higher for transients and harmonics. Further, it assumes the periodicity of the signal by which accuracy of detection degrades. On the contrary, mathematical morphology deals with simple addition and subtraction of signals without undergoing multiplication and division. With a smaller data window, i.e., with the knowledge of a small portion of the signal, it is able to detect the abnormalities quickly and accurately. Dilation and erosion are two basic operations with which generalized open close operation can be explored. Erosion is a kind of shrinking transform, which can make the target signal contract with holes enlarging. Dually, dilation is an expanding process, which realizes the target signal, enlarging together with holes contracting. Generally, erosion and dilation are not reversible each other. So the conjugation of them can form new morphological operators, named by opening and closing, which are also important operators in mathematical morphology. Further, the choice of structural element should be optimum to enable better performance for the morphological filter [26], [27].

Consider $d_s(n)$ as a disturbance voltage signal, defined in domain $D_{d_s} = \{x_0, x_1, \ldots, x_n\}$, and $g_s(m)$ be the structuring element (SE) defined in domain $D_{g_s} = \{y_0, y_1, \ldots, y_m\}$, where n and m are integers, such that $n > m$. Then dilation (D) and erosion (E) of $d_s(n)$ by $g_s(m)$ are given as [25]

$$y_D(n) = (d_s \oplus g_s)(n) = \max\left\{\begin{matrix} d_s(n-m) + g_s(m) \\ 0 \le (n-m) \le n, m \ge 0 \end{matrix}\right\} \tag{13}$$

$$y_E(n) = (d_s \ominus g_s)(n) = \min\left\{\begin{matrix} d_s(n+m) - g_s(m) \\ 0 \le (n+m) \le n, m \ge 0 \end{matrix}\right\}. \tag{14}$$

Now, with the above dilation and erosion, two composite operations [opening (O) and closing (C)] are given as

$$y_O(n) = (d_s \circ g_s)(n) = ((d_s \ominus g_s) \oplus g_s)(n) \tag{15}$$

$$y_C(n) = (d_s \bullet g_s)(n) = ((d_s \oplus g_s) \ominus g_s)(n). \tag{16}$$

An SE is a function used as a probe to extract features, keeping details, and reducing noise from a signal. There is no specific rule for appropriate choice of SE. The length of SE depends upon the sampling period of the signal. If sampling rate increases, accordingly the length of SE will also increase, not strictly linearly [28]. Islanding being an online application, speed is always an important factor so that a quick response is governed in the detection of system disturbances. In a conventional opening–closing (OC) and closing–opening (CO) filter, there exists serious statistical deflection that influences noise suppression of morphological filter directly. Because of dissimilarity of expansion process in opening operation and contraction process in closing operation, overall filtering performance may not be good. In this context, in order to suppress noise and achieve better performance, a different SE is taken. To overcome this, generalized morphological filter is implemented for the detection application. The output of such filter

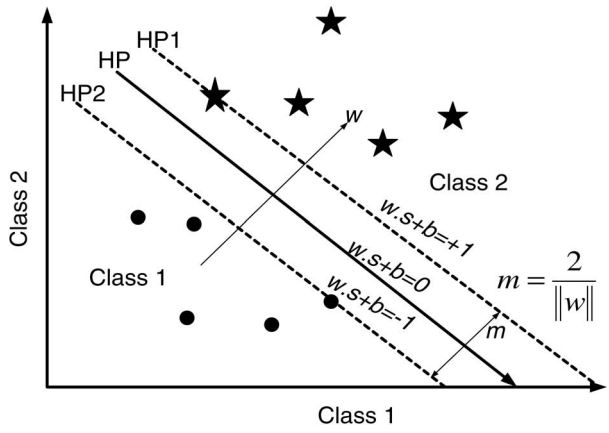

Fig. 3. Hyperplane for SVM.

depends upon proper choice of SE along with morphological transformation

$$F_{\mathrm{GOC}}(d_s(n)) = d_s \circ g_{s_1} \bullet g_{s_2}(n) \tag{17}$$

$$F_{\mathrm{GCO}}(d_s(n)) = d_s \bullet g_{s_1} \circ g_{s_2}(n) \tag{18}$$

where g_{s_1} and g_{s_2} are two SEs such that $g_{s_1} \subseteq g_{s_2}$. In the present study, g_{s_1} is linear and g_{s_2} is semicircular having length seven. This paper employs the difference in the generalized opening and closing, open, close erosion, and dilation, in order to detect any abnormality present in the signal

$$\left.\begin{matrix} \det_{\mathrm{GCO}}(n) = F_{\mathrm{GCO}}(d_s(n)) - F_{\mathrm{GOC}}(d_s(n)) \\ \det_{\mathrm{OC}}(n) = F_{\mathrm{CO}}(d_s(n)) - F_{\mathrm{OC}}(d_s(n)) \\ \det_{\mathrm{DE}}(n) = F_D(d_s(n)) - F_E(d_s(n)) \end{matrix}\right\}. \tag{19}$$

Thus, the difference in generalized open and close operation is implemented to detect islanding and PQ disturbances.

D. SVM

SVM utilizes a statistical learning technique which provides very good accuracy in high-dimensional feature spaces. The classification of patterns is based on structural risk minimization method. SVM provides improved generalization performance than other classical techniques, such as artificial neural networks (ANNs) and Bays classifier because its training is supported on a sequential minimization technique. This makes it suitable for the classification of islanding and different PQ disturbances [17].

For n-dimensional inputs $s_i (i = 1, 2, \ldots, M)$, M is the sample number fitting to class1 or class2 with outputs $o_i = 1$ for class1 and $o_i = -1$ for class2, correspondingly. The hyperplane is given as

$$f(s) = w^T s + b = \sum_{j=1}^{n} w_j s_j + b = 0 \tag{20}$$

where w is the n-dimensional vector and b is a parameter. The separating hyperplane position is defined by the w and b values as depicted in Fig. 3.

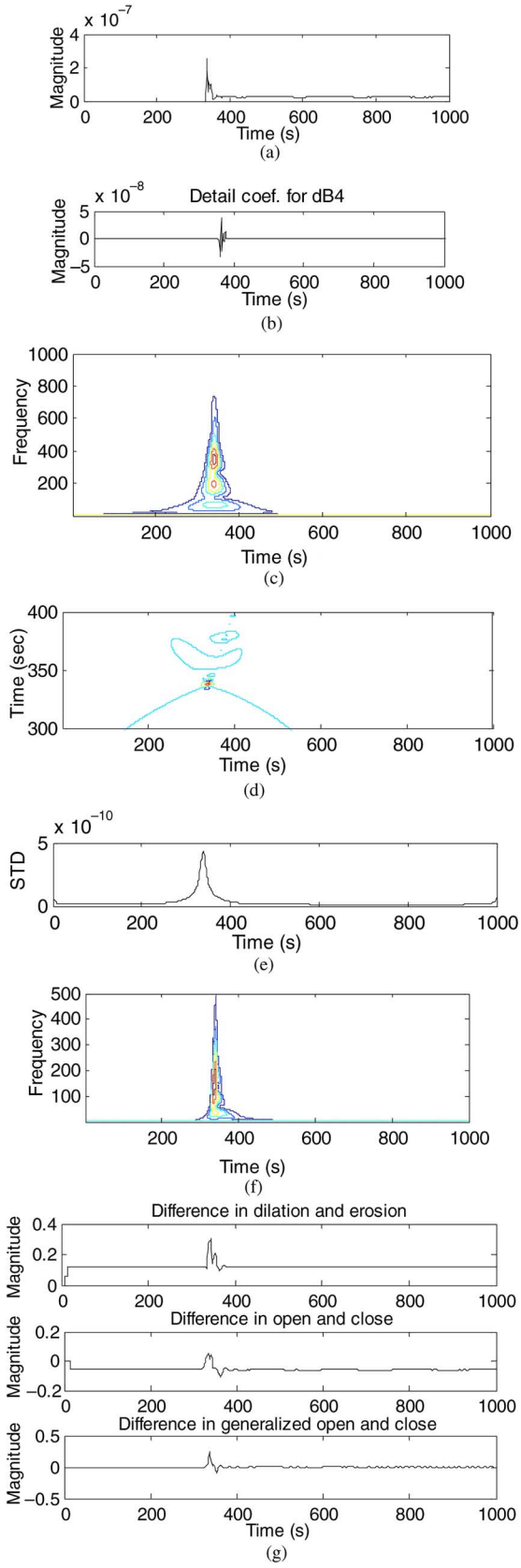

Fig. 4. Islanding detection event for the grid-connected wind energy system. (a) Negative sequence voltage at PCC of bus 13. (b) Detection using dB4 wavelet. (c) Detection using S-transform. (d) Detection using TTT. (e) STD profile using TTT. (f) Detection using HST. (g) Detection using mathematical morphology.

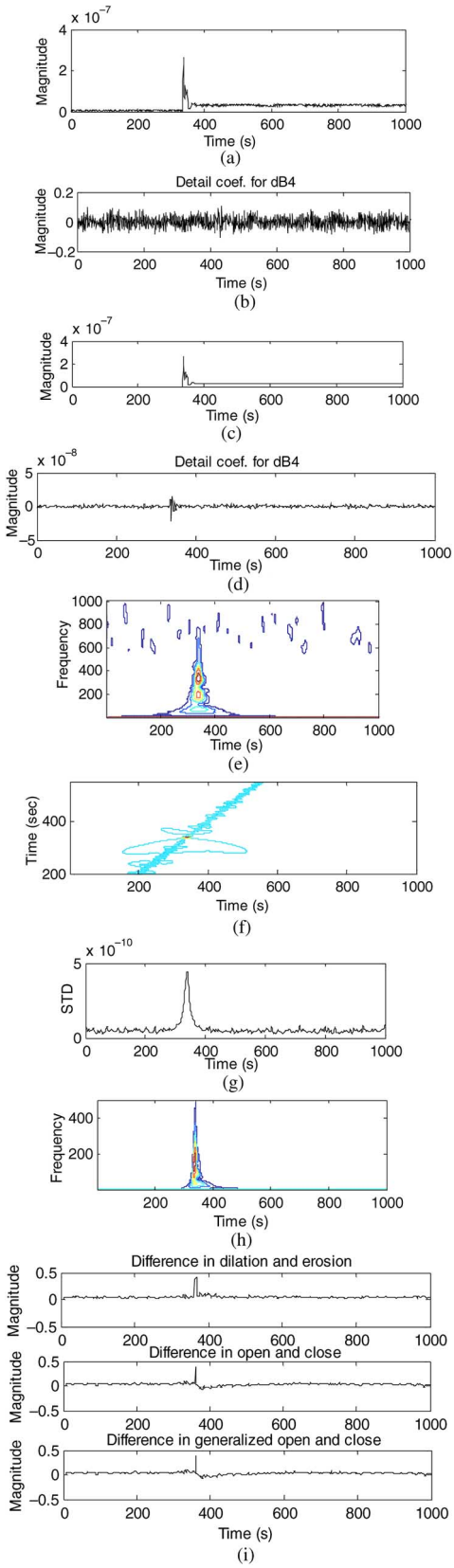

Fig. 5. Islanding detection event for the grid-connected wind energy system with 20-dB signal to noise ratio. (a) Negative sequence voltage. (b) Detection using dB4 wavelet. (c) De-noised negative sequence voltage. (d) Detection using dB4 wavelet de-noising. (e) Detection using S-transform. (f) Detection using TTT. (g) STD profile using TTT. (h) Detection using HST. (i) Detection using mathematical morphology.

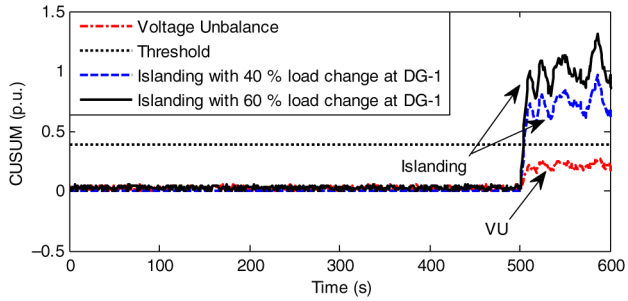

Fig. 6. CUSUM-based detection of VU and islanding events.

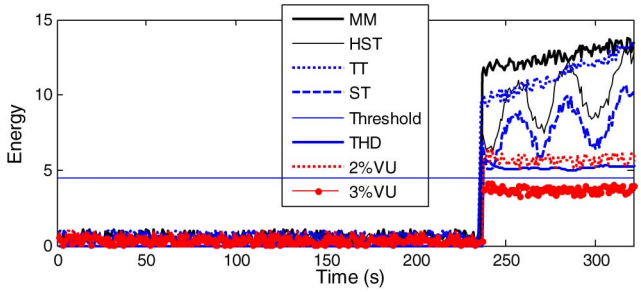

Fig. 7. Energy-based detection of islanding events.

The constraints are $f(s_i) \geq 1$, if $o_i = 1$ and $f(s_i) \geq -1$, if $o_i = -1$, thus

$$o_i f(s_i) = o_i(w^T s + b) \geq +1, \quad \text{for} \quad i = 1, 2, \ldots, M. \quad (21)$$

The geometrical distance is given as $||w||^{-2}$. The optimal hyperplane can be driven by the following optimization problem [25]:

$$\text{Minimize} \quad \frac{1}{2}||w||^{-2} + C\sum_{i=1}^{M}\xi_i \quad (22)$$

subject to

$$o_i(w^T s + b) \geq 1 - \xi_i, \quad \text{for} \quad i = 1, 2, \ldots, M \quad (23)$$

$$\xi_i \geq 0, \quad \text{for all } i. \quad (24)$$

The optimal bias value b^* is given as

$$b^* = -\frac{1}{2}\sum_{\text{SVs}} o_i \alpha_i^* (v_1^T s_i + v_2^T s_i) \quad (25)$$

where v_1 and v_2 are random SVM for class1 and class2, respectively.

The decision function corresponds to

$$f(s) = \sum_{\text{SVs}} \alpha_i o_i s_i^T s + b^*. \quad (26)$$

Unidentified data sample s is categorized as

$$s \in \left\{ \begin{matrix} \text{Class} - 1, \ f(s) \geq 0 \\ \text{Class} - 2, \ \text{otherwise} \end{matrix} \right\}. \quad (27)$$

The disturbances classification is accomplished applying a kernel function, such as Gaussian radial basis kernel function.

IV. Results and Discussion

Simulation results for the detection of islanding events in the hybrid DG system, using the above discussed techniques, are presented in this section under various operating scenarios. The operating scenarios for the grid-connected hybrid DG system are created in MATLAB/Simulink. The sampling rate in the simulations is 5 kHz with 50 Hz frequency.

The voltage signal at the point of common coupling (PCC), at different DG locations, is retrieved and processed through sequence analyzer to obtain its negative sequence component. The signals are then passed through the algorithms in order to detect and localize the islanding instants. The results of contour analysis by HST, TTT, and mathematical morphology are compared with the results obtained by using Daubechies 4 (dB4) as the mother wavelet and ST.

The quantitative analysis in terms of energy content, STD and CUSUM, of the transformed signal is also carried out in order to demonstrate the efficacy of the proposed detection techniques. The determination of the energy content of the transformed signal is based on "Parseval's theorem," which states that the energy of a signal $d_s(t)$ remains the same whether it is computed in a signal domain (time) or in a transform domain (frequency) [29]. Thus, the energy and STD of a signal is expressed as

$$E_{\text{signal}} = \frac{1}{T}\int_0^T |d_s(t)|^2 dt = \sum_{n=0}^{N} |d_s[n]|^2 \quad (28)$$

where T and N are the time period and the length of the signal, respectively, and $d_s[n]$ is the Fourier transform of the signal. Similarly, STD can be calculated from

$$\text{STD} = \left[\frac{1}{n}\sum_{i=1}^{n}(e_i - \bar{e})\right]^{1/2} \quad (29)$$

where n is the number of sample data and $e_i, \bar{e}$ are the voltage and mean of the voltage signal. CUSUM is computed by the sum of the consecutive samples of the energy of the voltage signal after being passed through different transforms. CUSUM of voltage signal is calculated as

$$\text{CUSUM}_v(p) = \sum_{1}^{r} E_{\text{vq}}(r) \quad (30)$$

where E_{vq} is the spectral energy of the negative sequence voltage signal at PCC and "r" is the length of signal over which energy and CUSUM are calculated, and "p" is the entire length of the signal.

The islanding event is detected when energy content/ STD/CUSUM becomes greater than a threshold value. The results presented in the following sections will clearly reflect the advantages of HST, TTT, and mathematical morphology over ST and WT in the detection of disturbances.

A. Islanding Detection for Grid-Connected Energy Resources

This subsection describes the detection using above described signal processing techniques.

TABLE I
CLASSIFICATION OF ISLANDING AND PQ DISTURBANCES BASED ON SVM

Islanding/PQ event	Classification accuracy using ST (%)				Classification accuracy using HST (%)				Classification accuracy using TTT (%)				Classification accuracy using MM (%)			
	Location				Location				Location				Location			
	DG1	DG2	DG3	DG4	DG1	DG2	DG3	DG4	DG1	DG2	DG3	DG4	DG1	DG2	DG3	DG4
Islanding	95.3	97.2	94.2	96.8	97.2	98.4	97.1	96.2	98.3	99.2	97.3	98.3	98.4	99.0	97.4	100
VU	94.9	95.4	97.1	96.2	95.3	97.1	97.0	95.0	97.4	97.3	98.2	97.6	99.2	98.2	97.0	99.0
Load switching	94.4	97.8	97.4	96.4	97.2	96.8	98.0	98.0	97.1	97.2	98.2	97.4	100	100	98.0	99.1
Notch with harmonics	97.2	96.2	95.8	97.2	96.6	97.3	96.4	97.6	98.5	98.4	99.5	98.0	100	99.0	99.0	98.0
Sag with harmonics	96.1	94.4	96.2	96.4	96.4	95.7	97.0	98.1	99.1	98.1	99.2	99.0	98.2	98.4	99.2	99.0
Swell with harmonics	96.5	94.6	97.2	95.6	98.1	96.2	98.2	97.8	97.2	97.2	98.6	98.0	99.1	98.0	100	99.4
Flicker	94.2	94.8	93.3	96.1	96.2	98.2	97.6	98.0	97.6	99.0	97.8	99.0	100	100	100	99.0
Oscillatory transient	96.6	96.3	95.0	96.5	98.7	97.5	96.0	97.0	99.2	97.1	99.0	97.3	100	99.0	100	100
Inrush	96.4	95.7	94.1	96.0	97.2	97.1	95.0	94.6	98.4	98.0	97.1	96.6	98.2	99.2	99.0	98.2

Fig. 4(a) shows the extracted negative sequence voltage signal at PCC13 (i.e., at bus 13), where DG3 is connected, when the wind energy system is suddenly disconnected from the grid. It is observed that islanding event occurs at around 350 sec. The detection using dB4 wavelet is shown in Fig. 4(b).

The detection using ST, TTT, HST, and mathematical morphology is shown in Fig. 4(c), (d), (f), and (g), respectively. These results clearly show a sudden increase in the magnitudes at the instant of islanding event, thus clearly localizing and detecting the disturbance.

The islanding detection in the same system with 20-dB signal to noise ratio is shown in Fig. 5.

Negative sequence voltage signal at PCC, at bus 13 where DG3 is connected, with 20-dB noise is shown in Fig. 5(a). It can be observed from the graphical results of Fig. 5(b) that the WT completely fails in the presence of noise, whereas, Fig. 5(c) and (d) show the de-noised negative sequence voltage signal and detection using WT, respectively. After de-noising, it is observed that the signal contains still some noise and as a result the detection using WT shows some deterioration. While ST shows the detection of islanding with an increased contour in Fig. 5(e), it is accompanied with scattered characteristic, i.e., deterioration in localization.

Hence, with ST, the detection process gets affected with some degradation with the increase in noise level in the voltage signal. The presence of noise obstructs an accurate detection, so these two techniques (wavelet and ST) are suggested to be noise sensitive.

Instead, as shown in Fig. 5(f)–(i), TTT, HST, and mathematical morphology are capable to detect and localize the islanding instant effectively. The transient noise characteristic leads to the appearance of bulge along the TT contours. Its STD value shows an apparent rise at the time of the islanding event.

The performance can also be presented quantitatively with the computation of performance indices: STD, energy content, and CUSUM [30], [31]. These features are the most distinguished ones for discriminating islanding events with those of nonislanding scenarios. A threshold is selected by comparing these indices for normal operating condition with that of the islanding event. The threshold value for the configuration in which all the resources (wind energy system, fuel cell, and photovoltaic system) are connected to the grid, is selected as 1.0145 for STD, 2.2314 p.u. for energy and 3.2546 for CUSUM by using HST. When the STD is more than 1.0145, energy content is more than 2.2314 p.u. and CUSUM is more than 3.2546, then the islanding event is detected; otherwise it corresponds to a PQ disturbance [18], [19].

The CUSUM-based detection is also tested on the IEEE 30-bus system, with disturbances in the form of islanding along with reduced 40% and 60% load change at PCC1 of DG1 location. Fig. 6 shows the discrimination of a 2% VU from islanding of DG1 location at bus 1 (including load) based on CUSUM, with selection of 0.411 as threshold value. Similarly, energy is considered as a common performance index in Fig. 7, which displays the performance of the proposed transforms/mathematical morphology (MM) along with conventional techniques such as THD and VU.

It is clear that indices value in case of THD and VU come nearer to the selected threshold, thereby increasing the chance of misdetecting islanding event, whereas, the indices value in case of proposed techniques come much higher with respect to the threshold value, proving the improvement in discriminating islanding from PQ disturbances. ST and HST show oscillations because of variations of frequency during disturbances and being time–frequency resolution analysis.

To augment this, the proposed transforms and SVM-based technique are used to classify islanding and different PQ disturbances, as shown in Table I. The voltage signal is passed through the transforms ST, HST, TTT, and MM, to find the feature dataset to be trained and tested by SVM in order to classify

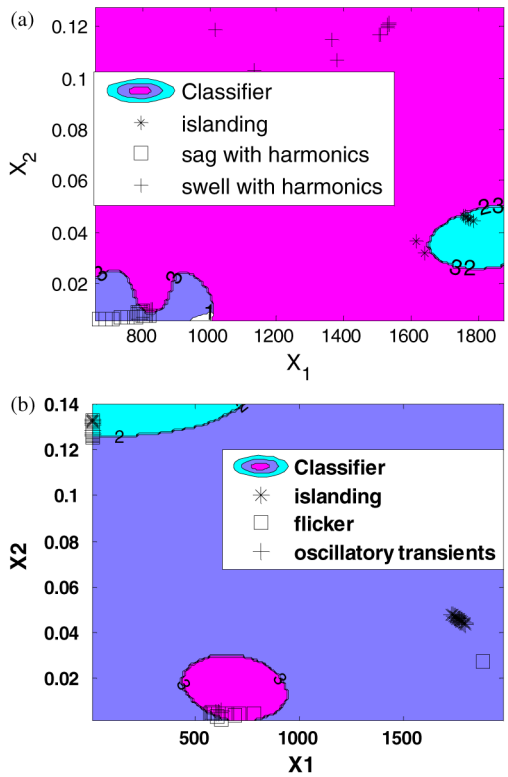

Fig. 8. Boundary plot for discriminating islanding and PQ. (a) Islanding versus sag with harmonics and swell with harmonics. (b) Islanding versus flicker and oscillatory transients.

all the disturbances. The features such as STD, energy, kurtosis, and skewness are selected and the procedure and parameters cited in [1] and [17] is followed for the classification objective.

The disturbances presented in Table I are created at different DG locations of the IEEE 30-bus system. Again, to support the classification of disturbances, boundary plots are shown in Fig. 8, which justify the discrimination of islanding from other PQ disturbances. Similarly, other disturbance's classification are studied using the above hybrid technique. A feature data matrix equal to 500×8 is formulated for all the disturbances, out of which half of the dataset is used for training and the remaining half for the testing of the SVM classifier.

The classification results given in Table I demonstrate that TTT and MM (being time–time transforms) show better accuracy than the time–frequency multiresolution analyses in the form of ST and HST. The detection time taken by different classification techniques, computed on Pentium-IV, 2.8 GHz, 1 GB RAM computer in MATLAB environment, is presented in Table II. It is observed that the detection time follows IEEE Std. 1547 in all cases. The islanding event occurs at bus 1, having DG1 connected and 2% VU in load is considered. In addition, detection time involved for other disturbances such as inrush, flicker, oscillatory transient, sag with harmonics are also given in that table.

B. *Effect of Harmonics on Islanding Detection*

This section describes the effect of harmonics presence in the voltage signal at PCC on the islanding detection (Fig. 9). The harmonics in the voltage waveform may be caused due

TABLE II
DETECTION TIME OF DIFFERENT TECHNIQUES

Detection technique	Disturbance/event	Time for detection (msec)
Wavelet	Islanding	25.0
	VU	28.0
	Inrush	27.4
	Flicker	29.1
	Oscillatory transient	28.7
	Sag with harmonics	26.9
S-transform	Islanding	26.0
	VU	27.0
	Inrush	28.8
	Flicker	27.7
	Oscillatory transient	28.6
	Sag with harmonics	28.1
HST	Islanding	22.0
	VU	23.0
	Inrush	24.3
	Flicker	23.7
	Oscillatory transient	24.6
	Sag with harmonics	23.3
TTT	Islanding	25.0
	VU	30.0
	Inrush	29.5
	Flicker	27.9
	Oscillatory transient	29.4
	Sag with harmonics	27.2
Mathematical morphology	Islanding	22.0
	VU	21.0
	Inrush	21.8
	Flicker	22.1
	Oscillatory transient	23.4
	Sag with harmonics	21.6

to the connection of nonlinear loads in the hybrid system. Harmonics, being a vital effect, must be eliminated because they lead to malfunctioning and failure of equipment, overheating, misdetection and misclassification of islanding and PQ problems, among others.

To test this effect, a nonlinear load is connected at PCC1, having DG1 connected, followed by islanding at the 825 sample. The corresponding voltage signal is as shown in Fig. 9(a). The increase in voltage in the form of a spike is observed due to islanding occurrence in addition to the presence of harmonics. This voltage signal is processed through WT, ST, HST, TTT, and mathematical morphology to detect the islanding event, shown in Fig. 9(b)–(d), (f), and (g), respectively. Fig. 9(e) represents the variation in STD due to islanding using TTT.

The results clearly show again that islanding detection completely fails using WT. Similarly, the detection is degraded to some extent in the case of ST. Instead, using HST, TTT, and mathematical morphology, islanding detection is observed to be much more effective and accurate even in the presence of harmonics.

With increased penetration of DG, the islanding and PQ issues become common occurrences that need to be analyzed by

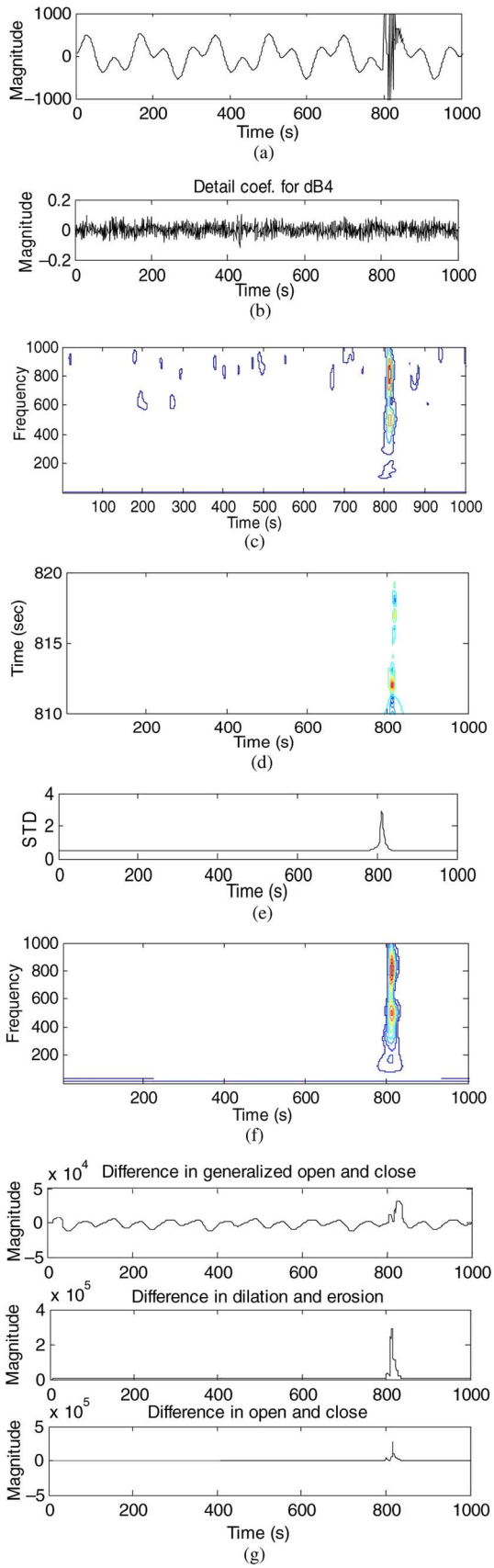

Fig. 9. Effect of harmonics on islanding detection. (a) Negative sequence voltage. (b) Detection using dB4 wavelet. (c) Detection using S-transform. (d) Detection using TTT. (e) STD profile using TTT. (f) Detection using HST. (g) Detection using mathematical morphology.

means of advanced signal processing techniques, as discussed in the introduction of the paper. The fast emergence of real-time processors these advanced signal processing techniques can be explored to accomplish disturbance detection. Accordingly, various hardware platforms, such as digital signal processing (DSP), field-programmable gate arrays (FPGAs), and/or LABVIEW, can be adopted in order to validate the correctness of the proposed method for the detection of islanding and PQ disturbance. Subsequently, the corrective action can be initiated to enhance the reliability of the system, which is indispensable.

V. Conclusion

This paper has presented a new study on the detection of islanding events in a grid-connected hybrid DG system using a plethora of techniques (WT, ST, HST, TTT, and mathematical morphology), under various operating scenarios. The performance of these approaches for islanding detection was tested and compared under different operating conditions. The contour analysis of HST/TTT and mathematical morphology techniques demonstrated their capability to clearly detect islanding events under both noise and noise-free conditions. Moreover, the presence of harmonics in the voltage signal confirmed the merits of HST, TTT, and mathematical morphology over WT and ST for the detection and localization of islanding events, which is an important characteristic. Further classification is accomplished with use of SVM in order to discriminate islanding with other PQ disturbances.

Acknowledgment

The authors acknowledge the support and facility available from the Department of Electrical Engineering, Motilal Nehru National Institute of Technology, Allahabad, India, for carrying out the research work.

References

[1] P. K. Ray, N. Kishor, and S. R. Mohanty, "Classification of power quality disturbances due to environmental characteristics in distributed generation system," *IEEE Trans. Sustain. Energy*, vol. 4, no. 2, pp. 302–313, Apr. 2013.

[2] O. C. Onara, M. Uzunoglu, and M. S. Alama, "Modeling, control and simulation of an autonomous wind turbine/photovoltaic/fuel cell/ultra-capacitor hybrid power system," *J. Power Sources*, vol. 185, no. 2, pp. 1273–1283, 2008.

[3] A. G. Tsikalakis and N. D. Hatziargyriou, "Operation of microgrids with demand side bidding and continuity of supply for critical loads," *Eur. Trans. Elect. Power*, vol. 21, no. 2, pp. 1238–1254, 2011.

[4] J. A. Pecas Lopes, N. Hatziargyriou, J. Mutale, P. Djapic, and N. Jenkins, "Integrating distributed generation into electric power systems: A review of drivers, challenges and opportunities," *Elect. Power Syst. Res.*, vol. 77, no. 9, pp. 1189–1203, 2007.

[5] H. Wang, F. Lui, Y. Kang, J. Chen, and X. Wei, "Experimental investigation on non detection zones of active frequency drift method for anti-islanding," in *Proc. 33rd Annu. Conf. IEEE Ind. Electron. Soc.*, Nov. 5–8, 2007, pp. 1708–1713.

[6] F. Liu, X. Lin, Y. Kang, Y. Zhang, and S. Duan, "An active islanding detection method for grid-connected converters," in *Proc. 3rd IEEE Int. Conf. Ind. Electron. Appl.*, Jun. 3–5, 2008, pp. 734–737.

[7] V. Menon and M. H. Nehrir, "A hybrid islanding detection technique using voltage unbalance and frequency set point," *IEEE Trans. Power Syst.*, vol. 22, no. 1, pp. 442–448, Feb. 2007.

[8] S. Jang and K. Kim, "An islanding detection method for distributed generation algorithm using voltage unbalance and total harmonic distortion of current," *IEEE Trans. Power Del.*, vol. 19, no. 2, pp. 745–752, Apr. 2004.

[9] H. H. Zeineldin, E. F. El-Saadany, and M. M. A. Salama, "Impact of DG interface control on islanding detection and non-detection zones," *IEEE Trans. Power Del.*, vol. 21, no. 3, pp. 1515–1523, Jul. 2006.

[10] H. H. Zeineldin and S. Kennedy, "Sandia frequency-shift parameter selection to eliminate non-detection zones," *IEEE Trans. Power Del.*, vol. 24, no. 1, pp. 486–487, Jan. 2009.

[11] H. H. Zeineldin and M. M. A. Salama, "Impact of load frequency dependence on the NDZ and performance of the SFS islanding detection method," *IEEE Trans. Ind. Electron.*, vol. 58, no. 1, pp. 139–146, Jan. 2011.

[12] K. El-Arroud, G. Joos, I. Kamwa, and D. T. McGillis, "Intelligent based approach to islanding detection in distributed generation," *IEEE Trans. Power Del.*, vol. 22, no. 2, pp. 828–835, Apr. 2007.

[13] N. W. A. Lidula and A. D. Rajapakse, "A pattern recognition approach for detecting power islands using transient signals—Part I: Design and implementation," *IEEE Trans. Power Del.*, vol. 25, no. 4, pp. 3070–3077, Oct. 2010.

[14] N. W. A. Lidula and A. D. Rajapakse, "A pattern recognition approach for detecting power islands using transient signals—Part II: Performance evaluation," *IEEE Trans. Power Del.*, vol. 27, no. 3, pp. 1071–1080, Jul. 2012.

[15] C.-T. Hsieh, J.-M. Lin, and S.-J. Huang, "Enhancement of islanding-detection of distributed generation systems via wavelet transform-based approaches," *Elect. Power Energy Syst.*, vol. 30, no. 10, pp. 575–580, 2008.

[16] M. Hanif, M. Basu, and K. Gaughan, "Development of EN50438 compliant wavelet-based islanding detection technique for three-phase static distributed generation systems," *IET Renew. Power Gener.*, vol. 6, no. 4, pp. 289–301, Jul. 2012.

[17] S. R. Mohanty, P. K. Ray, N. Kishor, and B. K. Panigrahi, "Classification of disturbances in hybrid DG system using modular PNN and SVM," *Elect. Power Energy Syst.*, vol. 44, no. 1, pp. 764–777, 2013.

[18] P. K. Ray, S. R. Mohanty, and N. Kishor, "Disturbance detection in grid connected distributed generation system using wavelet and S-transform," *Elect. Power Syst. Res.*, vol. 81, no. 3, pp. 805–819, 2011.

[19] P. K. Ray, N. Kishor, and S. R. Mohanty, "Islanding and power quality disturbance detection in grid-connected hybrid power system using wavelet and S-transform," *IEEE Trans. Smart Grid*, vol. 3, no. 3, pp. 1082–1094, Sep. 2012.

[20] P. K. Dash, B. K. Panigrahi, and G. Panda, "Power quality analysis using S–transform," *IEEE Trans. Power Del.*, vol. 18, no. 2, pp. 406–411, Apr. 2003.

[21] B. Biswal, P. K. Dash, and B. K. Panigrahi, "Non-stationary power signal processing for pattern recognition using HS-transform," *Appl. Soft Comput.*, vol. 9, no. 1, pp. 107–117, 2009.

[22] C. Simon, M. Schimmel, and J. J. Dañobeitia, "On the TT-transform and its diagonal elements," *IEEE Trans. Signal Process.*, vol. 56, no. 11, pp. 5709–5713, Nov. 2008.

[23] S. Suja and J. Jerome, "Pattern recognition of power signal disturbances using S transform and TT transform," *Elect. Power Energy Syst.*, vol. 32, no. 1, pp. 37–53, 2010.

[24] C. R. Pinnegar, "Time-frequency and time-time filtering with S Transform and TT transform," *Digit. Signal Process.*, vol. 15, no. 6, pp. 604–620, 2005.

[25] P. Li, J. Liu, X. Li, C. Tian, and J. Jie, "Detection of power quality disturbances in micro-grid based on generalized morphological filter and backward difference," in *Proc. 4th Int. Conf. Elect. Utility Deregul. Restruct. Power Technol. (DRPT)*, Jul. 6–9, 2011, pp. 1063–1066.

[26] S. Gautam and S. M. Brahma, "Overview of mathematical morphology in power systems-a tutorial approach," in *Proc. IEEE Power Eng. Soc. Gen. Meeting (PES'09)*, Calgary, AB, Canada, Jul. 26–30, 2009, pp. 1–7.

[27] S. Gautam and S. M. Brahma, "Out of step blocking function in a distance relay using mathematical morphology," *IET Gener. Transm. Distrib.*, vol. 6, no. 4, pp. 313–319, Apr. 2012.

[28] C. Xue *et al.*, "Power quality disturbance detect ion and location using mathematical morphology and complex wavelet transform," in *Proc. 3rd IEEE Conf. Ind. Electron. Appl.*, Jun. 3–5, 2008, pp. 2263–2268.

[29] A. M. Gargoom, N. Ertugrul, and W. L. Soong, "Automatic classification and characterization of power quality events," *IEEE Trans. Power Del.*, vol. 23, no. 4, pp. 2417–2425, Oct. 2008.

[30] S. R. Mohanty, A. K. Pradhan, and A. Routray, "Cumulative sum based fault detector for power system relaying application," *IEEE Trans. Power Del.*, vol. 23, no. 1, pp. 79–86, Jan. 2008.

[31] S. R. Samantaray, A. Samui, and B. C. Babu, "Time-frequency transform-based islanding detection in distributed generation," *IET Renew. Power Gener.*, vol. 5, no. 6, pp. 431–438, Nov. 2011.

Soumya R. Mohanty (M'08–SM'13) received the Ph.D. degree from Indian Institute of Technology (IIT), Kharagpur, India.

Currently, he is an Assistant Professor with the Department of Electrical Engineering, Motilal Nehru National Institute of Technology (MNNIT), Allahabad, India. His research interests include digital signal processing applications in power system relaying and power quality, and pattern recognition applications to distributed generation-based system.

Nand Kishor (SM'13) received the Ph.D. degree from Indian Institute of Technology (IIT), Roorkee, India.

Currently, he is an Associate Professor with the Department of Electrical Engineering, Motilal Nehru National Institute of Technology (MNNIT), Allahabad, India. Since August 2012, he has been working as a Marie Curie Experienced Researcher (Marie Curie Fellow) with the Electrical Engineering Department, Aalto University, Espoo, Finland. His research interests include artificial intelligence (AI) applications in power system, distributed generations, wireless sensor network, and digital signal processing applications in power system.

Prakash K. Ray (S'10–M'12) received the Ph.D. degree from Motilal Nehru National Institute of Technology (MNNIT), Allahabad, India.

Currently, he is working as an Assistant Professor with the Department of Electrical and Electronics Engineering, International Institute of Information Technology (IIIT), Bhubaneswar, India. His research interests include distributed generations, renewable energy resources, digital signal processing, and soft computing applications in power system.

João P. S. Catalão (M'04–SM'12) received the M.Sc. degree from the Instituto Superior Técnico (IST), Lisbon, Portugal, in 2003, and the Ph.D. degree and Habilitation for Full Professor ("Agregação") from the University of Beira Interior (UBI), Covilha, Portugal, in 2007 and 2013, respectively.

Currently, he is a Professor with UBI and Researcher at the Instituto de Engenharia de Sistemas e Computadores—Investigação e Desenvolvimento (INESC-ID), Lisbon, Portugal. He is the Primary Coordinator of the EU-funded FP7 project SiNGULAR ("Smart and Sustainable Insular Electricity Grids Under Large-Scale Renewable Integration"), a 5.2 million euro project involving 11 industry partners. He has published more than 95 journal papers, 175 conference proceedings papers and 12 book chapters, with an *h*-index of 21 (according to Google Scholar), having supervised more than 25 post-docs, Ph.D., and M.Sc. students. He is the Editor of the book entitled *Electric Power Systems: Advanced Forecasting Techniques and Optimal Generation Scheduling* (CRC Press, 2012) and translated into Chinese in January 2014. Currently, he is editing another book entitled *Smart and Sustainable Power Systems: Operations, Planning, and Economics of Insular Electricity Grids* (CRC Press, forthcoming). His research interests include power system operations and planning, hydro and thermal scheduling, wind and price forecasting, distributed renewable generation, demand response, and smart grids.

Prof. Catalão is the Editor of the IEEE TRANSACTIONS ON SUSTAINABLE ENERGY, Editor of the IEEE TRANSACTIONS ON SMART GRID, and Associate Editor of the *IET Renewable Power Generation*. He was the Guest Editor-in-Chief for the Special Section on "Real-Time Demand Response" of the IEEE TRANSACTIONS ON SMART GRID, published in December 2012, and he is currently Guest Editor-in-Chief for the Special Section on "Reserve and Flexibility for Handling Variability and Uncertainty of Renewable Generation" of the IEEE TRANSACTIONS ON SUSTAINABLE ENERGY. He is the recipient of the 2011 Scientific Merit Award UBI-FE/Santander Universities and the 2012 Scientific Award UTL/Santander Totta.